

Realization of a cavity-coupled Rydberg array

Jacopo De Santis,^{1, 2, 3, *} Balázs Dura-Kovács,^{1, 2, 3, *} Mehmet Öncü,^{1, 2, 3, *}
Adrien Bouscal,^{1, 2, 3, *} Dimitrios Vasileiadis,^{1, 3, 4} and Johannes Zeiher^{1, 2, 3}

¹Max-Planck-Institut für Quantenoptik, 85748 Garching, Germany

²Munich Center for Quantum Science and Technology (MCQST), 80799 Munich, Germany

³Fakultät für Physik, Ludwig-Maximilians-Universität, 80799 Munich, Germany

⁴Technische Universität München, TUM School of Natural Sciences, 85748 Garching, Germany

(Dated: February 13, 2026)

Scalable quantum computers and quantum networks require the combination of quantum processing nodes with efficient light-matter interfaces to distribute quantum information in local or long-distance quantum networks. Neutral-atom arrays have both been coupled to Rydberg states to enable high-fidelity quantum gates in universal processing architectures, and to optical cavities to realize interfaces to photons. However, combining these two capabilities and coupling atom arrays to highly excited Rydberg states in the mode of an optical cavity has been an outstanding challenge. Here we present a novel cavity-coupled Rydberg array that achieves this long-standing goal. We prepare, detect, and control individual atoms in a scalable optical tweezer array, couple them strongly to the optical mode of a high-finesse optical cavity and excite them in a controlled way to Rydberg states. We show that strong coupling to an optical cavity – demonstrated via the dispersive shift of the resonance of the cavity in presence of the atoms – and strong Rydberg interactions – demonstrated via the collective enhancement of Rydberg coupling in the atomic array – can be achieved in our setup at the same spatial location. Our presented experimental platform opens the path to several new directions, including the realization of quantum network nodes, quantum simulation of long-range interacting, open quantum systems and photonic-state engineering leveraging high-fidelity Rydberg control.

INTRODUCTION

The realization of efficient and high-quality interfaces between emitters and single photons is a central goal in quantum science [1], and an essential requirement for distributed quantum computing, metrology, or quantum communication, and ultimately a scalable quantum internet [2–4]. Optical cavities are a leading approach to achieving strong coupling between single atoms and single photons in the strong-coupling regime of cavity quantum electrodynamics (cQED) [5]. Single- or few-atom cavity-couplings have been leveraged to realize elementary atom-based building blocks of quantum networks, including fast non-destructive detection of atoms [6–8], the creation of entanglement between atoms [9–11] or the realization of photonic entangled states [12, 13]. Very recently, the capabilities of atomic cQED systems have been expanded by placing arrays of single atoms trapped in optical tweezers inside single-mode cavities [8, 14–19] or cavity arrays [20, 21]. In parallel, arrays of atoms coupled to highly excited Rydberg states have rapidly progressed, with advances in quantum computing, quantum simulation and quantum metrology [22, 23]. In particular, quantum computing based on neutral-atom arrays has become a central focus in the field, with breakthroughs in the realization of high-fidelity gates in different species and qubit implementations [24–28], excellent scalability of the array sizes [29–33] and first demonstrations of logical qubits and circuits [34–38].

Complementing the excellent control over individual qubits in Rydberg arrays with an efficient atom-light in-

terface featuring strong coupling between single atoms and single photons opens the path towards remote entanglement between nodes with computing capabilities, which is a cornerstone of scalable neutral-atom-based quantum network nodes [4, 39–41], smaller-scale logical quantum memories [42], and ultimately distributed quantum computing architectures [43–45]. Promising efforts towards the realization of such a hybrid platform include nano-photonic cavities [46, 47]. However, the strong electric fields in the vicinity of such devices have to be managed in order to generate Rydberg-based entanglement, which is limited to regions distant from the device [48]. In general, integrating high-fidelity Rydberg coupling with optical cavities poses challenges due to the presence of dielectric surfaces, e.g., in near-planar [10, 12, 13, 15] or fiber-based cavities [11, 49], or due to the electric field created by the required piezoelectric transducers, which are used to stabilize the length of optical cavities and ensure strong coupling to the atoms. While exciting progress has been made in photonic-state-engineering by ensembles coupled both to the modes of optical cavities and Rydberg states [50–52], these experiments typically do not operate in the single-atom cQED strong coupling regime and are lacking single-atom control. Up to now, it has been an outstanding challenge in the field to couple scalable arrays of single atoms to Rydberg states in or even near the mode of optical cavities.

Here, we overcome several experimental challenges and combine a tweezer array with individual atoms strongly coupled to the optical mode of a high-finesse optical cavity with Rydberg excitation. We prepare, detect, and

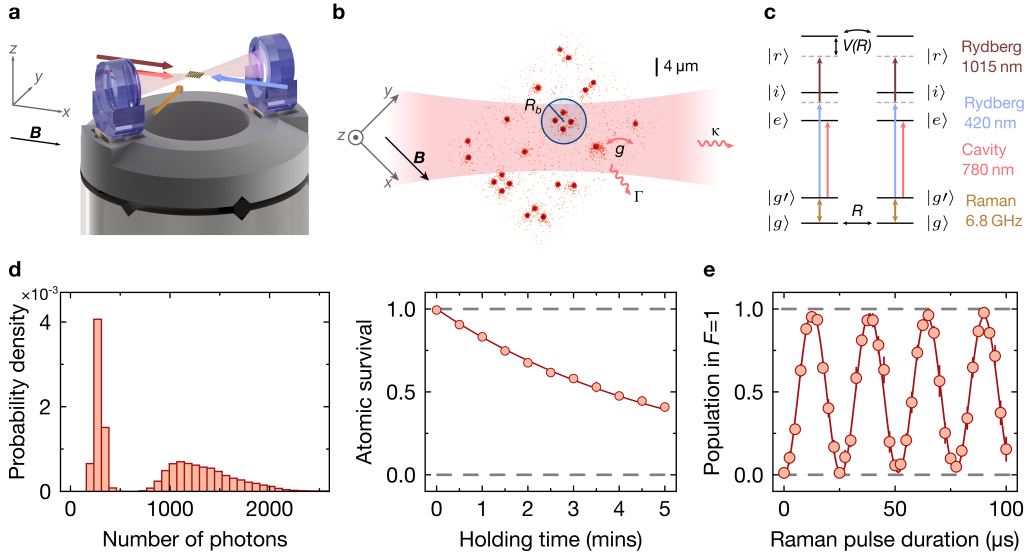


FIG. 1. Experimental setup and array generation. **a** Close-up of the optical cavity including the electric-field shielding platform, and atomic array. The counter-propagating dark red (blue) beams along the x -axis represent the 1015 nm (420 nm) components of the Rydberg excitation. The light red arrow represents the polarizer beam pumping to the state $|F = 2, m_F = -2\rangle$. The orange arrow represents the Raman beam. The light red shading between the mirrors denotes the cavity mode (not to scale). **b** Array of Rydberg-blockaded ensembles of 2×2 tweezers inside the cavity mode volume (red, not to scale), stochastically loaded with ^{87}Rb atoms. The magnetic quantization field is aligned with the x -axis. The Rydberg blockade disk is indicated in blue. The single-atom coupling to cavity mode g , the cavity decay rate κ , and the free-space atomic decay rate Γ are indicated. **c** Level diagram for two atoms, including the Raman, Rydberg, and cavity-coupling transitions. $|g'\rangle = |5\text{S}_{1/2}, F = 2, m_F = -2\rangle$, $|g\rangle = |5\text{S}_{1/2}, F = 1, m_F = -1\rangle$, $|e\rangle = |5\text{P}_{3/2}, F = 3\rangle$, $|i\rangle = |6\text{P}_{3/2}, F = 3\rangle$, $|r\rangle = |5\text{S}_{1/2}\rangle$. For a distance $R < R_b$, the Rydberg interaction energy shift V leads to Rydberg blockade. **d** Loading individual atoms in the optical traps, we perform high-fidelity (99.988(3)%)) and high-survival (99.88(2)%)) imaging with bimodal count histograms. Measurement of the loss dynamics of tweezer-trapped atoms yields a lifetime of 322(3) s. **e** Starting from atoms optically pumped to the state $|F = 2, m_F = -2\rangle$ using circularly polarized light, we demonstrate high-fidelity manipulations of the internal states of ^{87}Rb via a Raman beam detuned from the D1 line.

control individual atoms in a scalable optical tweezer array with up to 49 traps with high fidelities and couple them strongly to the mode of an optical cavity. We characterize the atom-cavity coupling via the dispersive atom-photon interaction when detuning the cavity from atomic resonance. Going beyond previous work, we controllably excite Rydberg states at the location of the cavity mode. In particular, we demonstrate that the transition frequency to Rydberg states is only minimally perturbed by the electric fields due to the cavity. Finally, we leverage the arbitrary configurability of the optical tweezers to prepare ensembles of up to four individual atoms in the regime of Rydberg blockade. Optically coupling these blockaded ensembles to a high-lying Rydberg state, we observe a square-root scaling of the Rabi frequency with atom number, a characteristic signature of entangled W-states expected in this regime [53, 54].

EXPERIMENTAL SETUP

Our experiments are performed in a new experimental machine based on ^{87}Rb atoms, optimized for combining

a tweezer array, a near-concentric optical cavity and Rydberg excitations; see Fig. 1a. Our tweezer arrays at a wavelength of 1015 nm are generated using a spatial light modulator, which enables arbitrary tweezer configurations via phase-only modulation [55]. The tweezers are focused in the atomic plane using a microscope objective with a numerical aperture (NA) of 0.6, resulting in arrays of up to 49 near diffraction-limited optical tweezers at the center of our optical cavity with a trap depth of approximately 1.2 mK. Fluorescence from the atoms is collected through the same objective and then delivered to a qCMOS camera, yielding a high-signal-to-noise image of individual atoms in the tweezer array for an exposure time of 80 ms; see Fig. 1b. By analyzing three subsequent images [31], we find initial loading probabilities of 52.0(2)%, imaging fidelities of 99.988(3)% and single-atom survival probabilities as high as 99.88(2)%, compatible with other results achieved in alkali atoms; see Fig. 1d. The high-finesse cavity is built in a near-concentric configuration, assembled from two mirrors with radius of curvature $R = 10$ mm each, and with a mirror separation of ~ 20 mm. This configuration maximizes optical access while simultaneously support-

ing small optical modes at the cavity center and hence large single-atom cooperativity $C = 4g^2/\kappa\Gamma$, where g denotes the vacuum Rabi coupling of the atom to the cavity mode, κ the decay rate of the photons out of the cavity, and Γ the decay rate of atoms due to photons emitted into free space [8, 14, 56, 57]. In addition to the cavity coupling, we can also controllably excite the atoms to Rydberg states on a two-photon transition via the intermediate $6P_{3/2}$ -state and at interatomic distances where Rydberg blockade is expected; see Fig. 1c. In order to ensure mechanical decoupling of the cavity from vibrations of the experimental table and the vacuum chamber, we mount the two mirrors on top of a mechanical vibration isolation tower; see Fig. 1a. The combination of stainless steel rings and an ultra-high vacuum compatible fluoroelastomer results in a strong low-passing character of the entire structure. The top part of the tower is manufactured from titanium, which features a low outgassing rate and thus enables long vacuum-limited lifetimes. In fact, we verify that we can hold the atoms in our tweezers under continuous cooling conditions for 322(3) s (see Fig. 1d), despite the vicinity of the glued cavity mirror assemblies. At the same time, the metallic titanium platform shields electric fields generated by the piezos used to stabilize the cavity length.

In order to demonstrate high-fidelity manipulation of the internal atomic states, we first optically pump the atoms to the state $|F = 2, m_F = -2\rangle$ using a σ^- -polarized beam aligned with the quantization axis (x -axis) and stabilized to the $F = 2 - F' = 2$ transition in ^{87}Rb . Subsequently, we drive the $|F = 1, m_F = -1\rangle$ to $|F = 2, m_F = -2\rangle$ transition using a Raman beam aligned with the y -axis, with an intermediate-state detuning of $\Delta_R = 2\pi \times 100$ GHz from the D1 line. The Raman system uses a combination of a chirped Bragg grating with an electro-optical modulator to generate efficient amplitude modulation [58]. We perform state-selective detection by removal of atoms in $F = 2$ to observe Rabi oscillations and thus arbitrary initial-state control at the single-qubit level when combined with phase-control on the Raman beam pair; see Fig. 1e. We also use the same Raman beam with a retroreflection mirror in order to drive motional sidebands of the atoms, allowing us to realize Raman sideband cooling down to average motional occupation of $\bar{n} = 0.62(15)$ in one dimension.

CAVITY COUPLING

After demonstrating the generation of tweezer arrays as well as high-fidelity preparation and manipulation of atoms, we proceed by showing that they strongly couple to the mode of the optical cavity. We first characterize the cavity without loading atoms using a 780 nm probe beam coupled into the cavity and detected in transmission using a single-photon counting module (SPCM). We

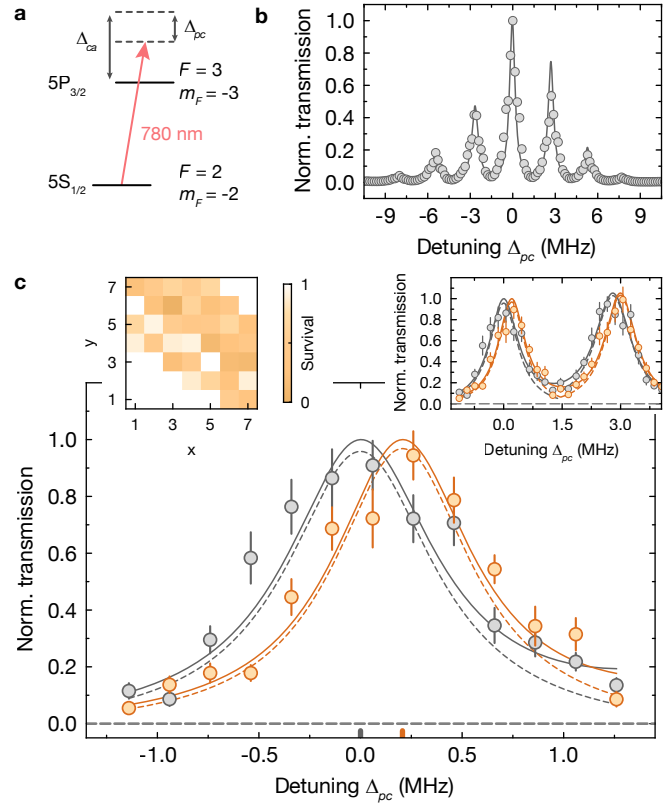


FIG. 2. Cavity geometry and atom-cavity interaction. **a** Relevant levels to probe the cavity spectrum. The probe beam, resonant with the cavity, is detuned from the D_2 -cycling transition by Δ_{ca} and the probe is varied around that point by Δ_{pc} . **b** Scanning the cavity resonance in the absence of atoms with the probe, we obtain a spectrum of the cavity modes. Instead of the expected single Lorentzian peak, we find a family of several lines split by approximately 3 MHz, which we attribute to mode hybridization as described in the main text. **c** Dispersive shift of the cavity resonance measured in the presence of atoms in the cavity (orange) compared with the empty cavity resonance (grey). The solid lines are the results of fitting a sum of Lorentzian peaks to the cavity transmission signal, taking into account the two dominant neighboring peaks (see right inset for a zoom out). The dashed line represents a single Lorentzian peak extracted from the fitted sum and used for estimating the cavity cooperativity. Orange (grey) ticks indicate the position of the cavity resonance with (without) atoms. The left inset shows the spatial structure of the mode as measured via the pushing effect on a 7×7 tweezer array at $\Delta_{ca} = \Delta_{pc} = 0$.

find a free-spectral range of $\text{FSR} = 7.79(2)$ GHz, consistent with the value calculated from the separation of the mirrors. Interestingly, when scanning a probe beam around the position of an expected cavity resonance ($\Delta_{pc} = 0$ in Fig. 2a), we observe a splitting of the cavity resonance into several modes separated by approximately 3 MHz, with a linewidth of each mode of $\kappa = 2\pi \times 0.84(9)$ MHz; see Fig. 2b. We attribute the structure to hybridization of low-order modes with

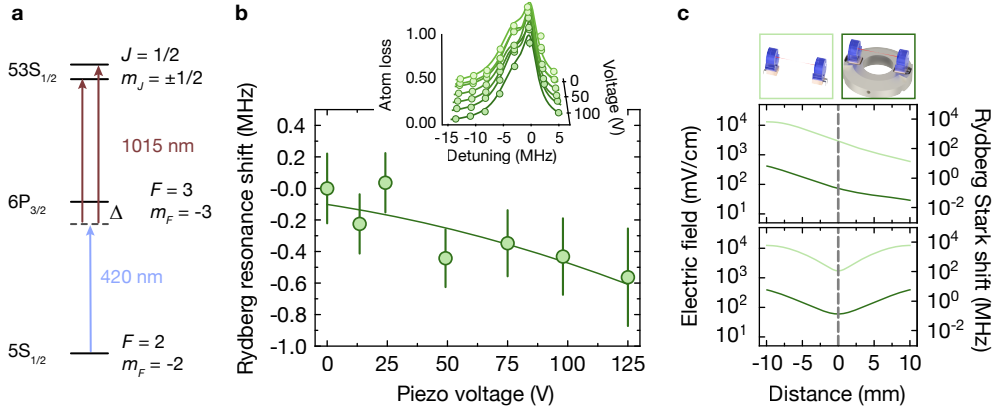


FIG. 3. **Electric field shielding.** **a** Rydberg excitation scheme. We couple the Rydberg state $53S_{1/2}$ starting from the ground state $5S_{1/2}$ via the intermediate state $6P_{3/2}$ with an intermediate-state detuning of $\Delta = 2\pi \times 2$ GHz via lasers at 420 nm and 1015 nm. **b** Measuring the Rydberg resonance as a function of the applied voltage to the piezos, we find only a weak shift that agrees well with our ab-initio modeling of the cavity assembly including the electric field shield (solid line). The inset shows the resonance scan at each piezo voltage from which we extract the shift. **c** Comparison of the electric field at the position of the atoms in a configuration where the mirrors sit on exposed piezos (light green) with our configuration where they are buried in a titanium platform (dark green). Top: Case where only one piezo is driven to 100 V. Bottom: Symmetric case where both piezos are driven. The weak dependence observed in **b** is hence a direct consequence of our shielding of the piezo. We find that a suppression of the electric field by more than one order of magnitude is achieved, which corresponds to close to three orders of magnitude suppression of the resonance shifts (right axis).

very high-order modes, which can occur due to non-paraxial effects in the cavity in combination with imperfect mirrors [59, 60]. Importantly, the optical profiles of the modes in this family are similar and well approximated by an elliptical Gaussian profile. Moreover, compared with the expected linewidth, we find a modest increase, which we attribute to slightly larger losses for the hybridized modes. While these effects reduce the expected atom-photon coupling, we calculate from the measured cavity mode profile, the measured linewidth, and the known atomic decay an expected cooperativity of $C_{\text{th}} = 1.06(12)$ in the strong cQED single-atom coupling regime. We verify this prediction experimentally by preparing a tweezer array with 7×7 traps loaded stochastically with single atoms in the optical cavity. To center the cavity mode on the tweezer array, we initially keep the cavity resonant with the atomic cycling transition $F = 2 - F' = 3$ in ^{87}Rb , i.e., setting the atom-cavity detuning $\Delta_{\text{ac}} = 0$; see Fig. 2a. We then lower the tweezers to a depth of 0.3 mK and couple resonant probe light into the cavity mode, which locally heats the atoms in the tweezer array and leads to atom loss at the position of the optical mode; see inset of Fig. 2c. The cavity is kept resonant with the atomic transition by locking it to a stabilized laser at 840 nm. After completing the alignment of the array with the cavity mode, we detune the cavity resonance from atomic resonance by $\Delta_{\text{ac}} = 2\pi \times 73.2(4)$ MHz and reduce the probe power coupled into the cavity. In this configuration, the atoms couple dispersively to the cavity resonance, leading to an expected atom-number dependent shift of the cavity res-

onance given by $\delta_N = NC(\Gamma\kappa/4\Delta_{\text{ac}}) = N(g^2/\Delta_{\text{ac}})$ [56]. The cavity resonance shift is measured by scanning the probe beam across the cavity resonance; see Fig. 2c. Here, every data point is obtained after probing the cavity at the given Δ_{pc} for an exposure time of 100 μs . We find an overall shift of $\delta_N = 2\pi \times 206(56)$ kHz for an average of $\bar{N} = 23.3(4)$ atoms coupled to the cavity mode. Under the approximation of homogeneous coupling of all trapped atoms to the mode, we extract the average single-atom dispersive shift of the cavity resonance of $\delta_1 = 2\pi \times 9(3)$ kHz. This yields an estimate for the single-atom cooperativity of $C = 0.51(18)$. We note that, in our current geometry, the extracted cooperativity underestimates the true cooperativity of the cavity by at least a factor of 2.5 due to the spatial mode profile of the cavity: the Gaussian cavity mode profile leads to a reduced coupling of atoms off-center and the atom positions are not fine-tuned to be aligned with the maxima of the standing wave within the cavity [61]. Taking this factor into account, we conclude that our cavity operates in the strong cQED coupling regime $C \approx 1$.

RYDBERG RESONANCE

Exciting Rydberg atoms in the cavity poses a substantial challenge due to the vicinity of the dielectric cavity mirror substrates as well as the piezoelectric transducers required to control the length of the cavity. In our near-concentric cavity geometry, effects coming from the mirror surfaces are expected to be small due to the large

mirror separation. However, voltages of up to 125 V may be applied at the piezos at a distance of approximately 10 mm from the location of the tweezer array and the cavity mode. Rydberg states can couple to this electric field via their strong DC-polarizability, which results in detrimental, fluctuating resonances and long-term drifts at a scale of up to 1 GHz. Conversely, exciting Rydberg atoms enables precise probing of the local electric field environment at the location of the atoms [62, 63]. To characterize the effectiveness of our titanium platform to shield electric fields generated by the piezos, we couple to the state $53S_{1/2}$ starting from the $5S_{1/2}$ ground state. We employ an off-resonant two-photon excitation from the intermediate $6P_{3/2}$ state involving a blue photon at 420 nm on the lower leg and a near-infrared photon at 1015 nm on the upper leg; see Fig. 3a. Due to imperfect polarization, we observe an asymmetric resonance peak with both the $m_J = \pm 1/2$ sublevels of the Rydberg manifold appearing; see inset of Fig. 3b. Tracking the position of the resonance as function of the applied voltage to the piezo, we find only a small shift of approximately 400 kHz for voltages up to 125 V, in line with the expectation obtained from a finite-element simulation of the electric field configuration at the location of the atoms. This strong suppression of the electric field is further illustrated in Fig. 3c by simulations comparing the field as a function of the distance from the piezo in the cases of shielded and unshielded piezos. We find that our simple design of burying the piezo in the metallic titanium platform leads to a suppression of the electric field at the position of atoms by more than one order of magnitude, resulting in a reduction of the expected resonance shifts from the 100 MHz-range to a few 100 kHz. Furthermore, we note that it is unlikely that applying voltages as high as 125 V will be required to keep the cavity at the working point. In fact, we have confirmed that long term drifts of the cavity resonance can be compensated by controlled heating of the cavity mounts, allowing the piezos to always work in the same limited voltage range. We anticipate that the small modulations required on top of such a large, thermally regulated cavity length, will render fluctuations of the Rydberg resonance completely irrelevant.

COLLECTIVE RABI OSCILLATIONS

With stable Rydberg resonances established, we finally demonstrate the controlled excitation of Rydberg states in an interacting regime at the location of the cavity mode. Specifically, we adapt the tweezer pattern to feature groups of atoms separated by approximately 2.5 μm , within the expected blockade radius of $R_b = 4.8 \mu\text{m}$ for the Rydberg state $53S_{1/2}$. When suddenly switching on the Rydberg coupling under these conditions, we find coherent Rabi oscillations between the ground and Ryd-

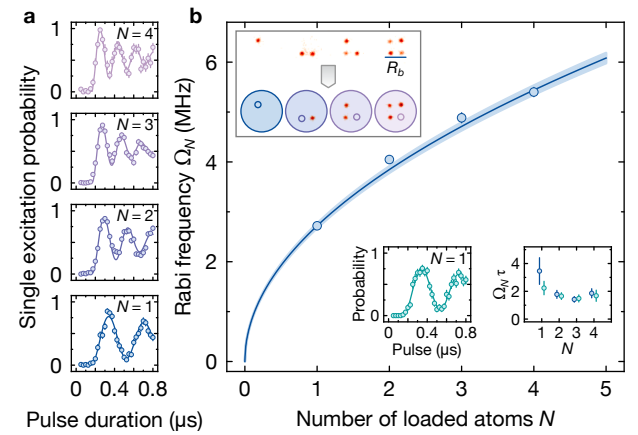


FIG. 4. **Collective Rydberg coupling.** **a** Preparing a tweezer array with groups of four tweezers within a Rydberg blockade radius $R_b = 4.8 \mu\text{m}$, indicated by the radius of the circle in the inset in **b**, we measure the probability of finding maximally one excitation in the system after suddenly turning on the Rydberg coupling light (blue points). When postselecting on the initially prepared number of atoms, N , we find that the Rabi frequency increases with atom number, as extracted from a sinusoidal fit of the form $A(1 - e^{-(t-t_0)/\tilde{\tau}} \cos(\tilde{\Omega}(t-t_0) + \phi))$. **b** We find quantitative agreement with the expected dependence of the extracted Rabi frequency (blue points) with a prediction based on scaling the extracted Rabi frequency Ω for $N = 1$ with the square-root of the number of atoms within a blockade radius, $\Omega_N = \Omega\sqrt{N}$ (solid line). The left panel in the inset shows the Rabi oscillations in the presence of a full-amplitude piezo scan (cyan datapoints), together with a fit (solid line). The right panel shows the extracted “quality factor” $\Omega_N\tau$ without (with) scanning the piezos in blue (cyan). We find no difference between the two cases within errorbar.

berg states, which are not trapped and thus lost from our tweezers before detection. We group the data according to the atom number obtained from a first image taken before the Rydberg excitation. Limiting the maximal number of lost atoms to one in a second image after the dynamics, we extract the probability of creating a single Rydberg excitation, depending on the initial atom number; see Fig. 4a. Double Rydberg excitation due to imperfect blockade or atom loss in the tweezers due to heating lead to a small fraction of less than 3% of the events where two or more atoms are lost. Fitting a damped oscillation to the data for $N = 1$ atom per group, we extract $\Omega = 2\pi \times 2.72(5)$ MHz. Furthermore, we find that the Rabi frequency increases with the initial atom number N in a four-tweezer group with a characteristic dependence of the coupling strength, $\Omega_N = \sqrt{N}\Omega$, signaling the coupling to the multi-partite entangled W-state [53, 54]; see Fig. 4b. To verify the minimal impact of the electric field also in this Rabi oscillation measurement, we perform the same sequence while scanning the cavity piezos by ± 65 V with a triangle ramp at a fre-

quency of 1.1 kHz. Extracting the dephasing time of the Rabi oscillations τ , we find that the “quality factor” $\Omega_N\tau$, i.e. the number of coherent oscillations per decay time is, within errorbar, indistinguishable between scanned and unscanned case despite the large scanning amplitude.

CONCLUSION

In summary, we have presented a new experimental setup that combines single tweezer-trapped atoms with a high-finesse optical cavity and highly excited Rydberg states. Our results clearly demonstrate the compatibility of these capabilities, which will be further enhanced with several planned improvements that will be implemented in the near future. First, we are currently preparing an upgraded version of our optical cavity, which, together with more precise control over the tweezer positions, will boost our single-atom cooperativity by at least one order of magnitude by mitigating the observed mode-hybridization. Second, we are working on a phase-noise reduction system for our Rydberg excitation beam at 1015 nm, which is currently derived from an extended-cavity diode laser locked to an ultralow expansion glass cavity. We expect that the suppression of phase noise in the MHz-regime will effectively mitigate the observed dephasing in the Rydberg Rabi oscillations [64–66], opening a straightforward path towards high-fidelity two-qubit gate operations on the ground-state qubits. Already with the currently achieved parameters, our setup opens the route to a number of interesting directions, including the realization of cavity-assisted non-destructive readout [8] and cyclic error correction codes prepared using high-fidelity Rydberg coupling [34, 38]. Fast, non-destructive readout combined with high-fidelity preparation of entangled states could also be used to realize one-way-quantum computing [67]. The non-local connectivity provided by the cavity opens the route towards novel two-qubit gate schemes [68–71] that could overcome the time-overhead of shuttling qubits over large distances within a node by asynchronous entanglement distribution. Furthermore, leveraging the high-fidelity entangling gates of atom arrays coupled to the optical cavity, we anticipate applications in photonic state engineering, where atomic entanglement is repeatedly swapped to photonic states [13, 72, 73], thus paving the way for novel quantum network [4, 41] and distributed quantum computing [42] protocols. Finally, our system opens a new direction in analog and mixed analog-digital quantum simulations where strong Rydberg interactions compete with long-range cavity interactions and dissipation. Such a setting features a rich and experimentally largely unexplored phase diagram [74, 75], novel out-of-equilibrium dynamics [76, 77], as well as novel routes to engineer interesting entangled states within the cavity [78].

We acknowledge helpful discussions with Tracy

Northup, Dan Stamper-Kurn, and Darrick Chang and their teams. We are grateful to Pranav Kulkarni, Sebastian Ruffert, Miriam Keim, Mullai Sampangi, and Arda Özkut for early contributions to the experimental setup. We thank Maximilian Ammenwerth for feedback on the manuscript. We acknowledge funding by the Deutsche Forschungsgemeinschaft (DFG, German Research Foundation) under Germany’s Excellence Strategy—EXC-2111-390814868 (MCQST), from the Munich Quantum Valley initiative as part of the High-Tech Agenda Plus of the Bavarian State Government, and from the BMFTR through the program “Quantum technologies—from basic research to market” (SNAQC, Grant No. 13N16265). We also acknowledge funding through JST-DFG 2024: Japanese-German Joint Call for Proposals on “Quantum Technologies” (Japan-JST-DFG-ASPIRE 2024) under DFG Grant No. 554561799. J.D.S, B.D.K, and M.Ö acknowledge funding from the International Max Planck Research School (IMPRS) for Quantum Science and Technology. A.B acknowledges support through a fellowship from the Alexander von Humboldt Foundation.

* These authors contributed equally to this work.

- [1] D. E. Chang, V. Vuletić, and M. D. Lukin, Quantum nonlinear optics — photon by photon, *Nature Photonics* **8**, 685 (2014).
- [2] H. J. Kimble, The quantum internet, *Nature* **453**, 1023 (2008).
- [3] S. Wehner, D. Elkouss, and R. Hanson, Quantum internet: A vision for the road ahead, *Science* **362**, eaam9288 (2018).
- [4] J. P. Covey, H. Weinfurter, and H. Bernien, Quantum networks with neutral atom processing nodes, *npj Quantum Information* **9**, 90 (2023).
- [5] A. Reiserer and G. Rempe, Cavity-based quantum networks with single atoms and optical photons, *Reviews of Modern Physics* **87**, 1379 (2015).
- [6] J. Bochmann, M. Mücke, C. Guhl, S. Ritter, G. Rempe, and D. L. Moehring, Lossless State Detection of Single Neutral Atoms, *Physical Review Letters* **104**, 203601 (2010).
- [7] J. Volz, R. Gehr, G. Dubois, J. Estève, and J. Reichel, Measurement of the internal state of a single atom without energy exchange, *Nature* **475**, 210 (2011).
- [8] E. Deist, Y.-H. Lu, J. Ho, M. K. Pasha, J. Zeiher, Z. Yan, and D. M. Stamper-Kurn, Mid-Circuit Cavity Measurement in a Neutral Atom Array, *Physical Review Letters* **129**, 203602 (2022).
- [9] S. Welte, B. Hacker, S. Daiss, S. Ritter, and G. Rempe, Photon-Mediated Quantum Gate between Two Neutral Atoms in an Optical Cavity, *Physical Review X* **8**, 011018 (2018).
- [10] S. Daiss, S. Langenfeld, S. Welte, E. Distante, P. Thomas, L. Hartung, O. Morin, and G. Rempe, A quantum-logic gate between distant quantum-network modules, *Science* **371**, 614 (2021).

[11] B. Grinkemeyer, E. Guardado-Sánchez, I. Dimitrova, D. Shchepanovich, G. E. Mandopoulou, J. Borregaard, V. Vuletić, and M. D. Lukin, Error-detected quantum operations with neutral atoms mediated by an optical cavity, *Science* **387**, 1301 (2025).

[12] P. Thomas, L. Ruscio, O. Morin, and G. Rempe, Efficient generation of entangled multiphoton graph states from a single atom, *Nature* **608**, 677 (2022).

[13] P. Thomas, L. Ruscio, O. Morin, and G. Rempe, Fusion of deterministically generated photonic graph states, *Nature* **629**, 567 (2024).

[14] E. Deist, J. A. Gerber, Y.-H. Lu, J. Zeiher, and D. M. Stamper-Kurn, Superresolution Microscopy of Optical Fields Using Tweezer-Trapped Single Atoms, *Physical Review Letters* **128**, 083201 (2022).

[15] L. Hartung, M. Seubert, S. Welte, E. Distante, and G. Rempe, A quantum-network register assembled with optical tweezers in an optical cavity, *Science* **385**, 179 (2024).

[16] J. Ho, Y.-H. Lu, T. Xiang, C. C. Rusconi, S. J. Masson, A. Asenjo-Garcia, Z. Yan, and D. M. Stamper-Kurn, Optomechanical self-organization in a mesoscopic atom array, *Nature Physics* **21**, 1071 (2025).

[17] Z. Wang, S. Guan, G. Teng, P. Yang, P. Zhang, G. Li, and T. Zhang, A cavity qed system with defect-free single-atom array strongly coupled to an optical cavity, *Quantum Frontiers* **4**, 10 (2025).

[18] B. Hu, J. Sinclair, E. Bytyqi, M. Chong, A. Rudelis, J. Ramette, Z. Vendeiro, and V. Vuletić, Site-Selective Cavity Readout and Classical Error Correction of a 5-Bit Atomic Register, *Physical Review Letters* **134**, 120801 (2025).

[19] M. L. Peters, G. Wang, D. C. Spierings, N. Drucker, B. Hu, M.-W. Chen, Y.-T. Chen, and V. Vuletić, Cavity-Enabled Real-Time Observation of Individual Atomic Collisions, *Physical Review Letters* **135**, 093402 (2025).

[20] A. L. Shaw, A. Soper, D. Shadmany, A. Kumar, L. Palm, D.-Y. Koh, V. Kaxiras, L. Taneja, M. Jaffe, D. I. Schuster, and J. Simon, A cavity-array microscope for parallel single-atom interfacing, *Nature* **650**, 320 (2026).

[21] A. Soper, D. Shadmany, A. L. Shaw, L. Palm, D. I. Schuster, and J. Simon, Stability, degeneracy, and scalability of a 600-site cavity array microscope, *arXiv:2602.06587* (2026).

[22] A. Browaeys and T. Lahaye, Many-body physics with individually controlled Rydberg atoms, *Nature Physics* **16**, 132 (2020).

[23] A. M. Kaufman and K.-K. Ni, Quantum science with optical tweezer arrays of ultracold atoms and molecules, *Nature Physics* **17**, 1324 (2021).

[24] S. J. Evered, D. Bluvstein, M. Kalinowski, S. Ebadi, T. Manovitz, H. Zhou, S. H. Li, A. A. Geim, T. T. Wang, N. Maskara, H. Levine, G. Semeghini, M. Greiner, V. Vuletić, and M. D. Lukin, High-fidelity parallel entangling gates on a neutral-atom quantum computer, *Nature* **622**, 268 (2023).

[25] J. A. Muniz, M. Stone, D. T. Stack, M. Jaffe, J. M. Kindem, *et al.*, High-fidelity universal gates in the ^{171}Yb ground state nuclear spin qubit, *PRX Quantum* **6**, 020334 (2025).

[26] M. Peper, Y. Li, D. Y. Knapp, M. Bileska, S. Ma, G. Liu, P. Peng, B. Zhang, S. P. Horvath, A. P. Burgers, and J. D. Thompson, Spectroscopy and Modeling of ^{171}Yb Rydberg States for High-Fidelity Two-Qubit Gates, *Physical Review X* **15**, 011009 (2025).

[27] R. Tao, O. Lib, F. Gyger, H. Timme, M. Ammenwerth, I. Bloch, and J. Zeiher, Universal gates for a metastable qubit in strontium-88, *arXiv:2506.10714* (2025).

[28] A. Senoo, A. Baumgärtner, J. W. Lis, G. M. Vaidya, Z. Zeng, G. Giudici, H. Pichler, and A. M. Kaufman, High-fidelity entanglement and coherent multi-qubit mapping in an atom array, *arXiv:2506.13632* (2025).

[29] F. Gyger, M. Ammenwerth, R. Tao, H. Timme, S. Snigirev, I. Bloch, and J. Zeiher, Continuous operation of large-scale atom arrays in optical lattices, *Physical Review Research* **6**, 033104 (2024).

[30] M. A. Norcia, H. Kim, W. B. Cairncross, M. Stone, A. Ryou, *et al.*, Iterative Assembly of ^{171}Yb Atom Arrays with Cavity-Enhanced Optical Lattices, *PRX Quantum* **5**, 030316 (2024).

[31] H. J. Manetsch, G. Nomura, E. Bataille, X. Lv, K. H. Leung, and M. Endres, A tweezer array with 6,100 highly coherent atomic qubits, *Nature* **647**, 60 (2025).

[32] N.-C. Chiu, E. C. Trapp, J. Guo, M. H. Abobeih, L. M. Stewart, *et al.*, Continuous operation of a coherent 3,000-qubit system, *Nature* **646**, 1075 (2025).

[33] J. Zhu, C. Chen, L. Zhou, X. Xie, C. Jiang, Z. Ding, F. Wu, F. Yang, G. Wang, Q. Gong, P. Zhang, S. Zhang, and P. Peng, High-efficiency loading of 2,400 ytterbium atoms in optical tweezer arrays, *arXiv:2512.19795* (2025).

[34] D. Bluvstein, S. J. Evered, A. A. Geim, S. H. Li, H. Zhou, *et al.*, Logical quantum processor based on reconfigurable atom arrays, *Nature* **626**, 58 (2024).

[35] B. W. Reichardt, A. Paetznick, D. Aasen, I. Basov, J. M. Bello-Rivas, *et al.*, Logical computation demonstrated with a neutral atom quantum processor, *arXiv:2411.11822* (2024).

[36] B. Zhang, G. Liu, G. Bernet, S. P. Horvath, P. Peng, S. Ma, S. Huang, S. Puri, and J. D. Thompson, Leveraging erasure errors in logical qubits with metastable ^{171}Yb atoms, *arXiv:2506.13724* (2025).

[37] R. Rines, B. Hall, M. H. Teo, J. Viszlai, D. C. Cole, *et al.*, Demonstration of a Logical Architecture Uniting Motion and In-Place Entanglement: Shor's Algorithm, Constant-Depth CNOT Ladder, and Many-Hypercube Code, *arXiv:2509.13247* (2025).

[38] D. Bluvstein, A. A. Geim, S. H. Li, S. J. Evered, J. P. Bonilla Ataides, *et al.*, A fault-tolerant neutral-atom architecture for universal quantum computation, *Nature* **649**, 39 (2026).

[39] A. Reiserer, *Colloquium: Cavity-enhanced quantum network nodes*, *Reviews of Modern Physics* **94**, 041003 (2022).

[40] W. Huie, S. G. Menon, H. Bernien, and J. P. Covey, Multiplexed telecommunication-band quantum networking with atom arrays in optical cavities, *Physical Review Research* **3**, 043154 (2021).

[41] Y.-L. Zhang, Q.-X. Jie, M. Li, S.-H. Wu, Z.-B. Wang, X.-B. Zou, P.-F. Zhang, G. Li, T. Zhang, G.-C. Guo, and C.-L. Zou, Architecture for a quantum repeater based on rydberg-atom quantum processors, *Phys. Rev. Appl.* **24**, 024052 (2025).

[42] J. Sinclair, J. Ramette, B. Grinkemeyer, D. Bluvstein, M. D. Lukin, and V. Vuletić, Fault-tolerant optical interconnects for neutral-atom arrays, *Physical Review Research* **7**, 013313 (2025).

[43] C. Monroe, R. Raussendorf, A. Ruthven, K. R. Brown, P. Maunz, L.-M. Duan, and J. Kim, Large-scale modular quantum-computer architecture with atomic memory and photonic interconnects, *Physical Review A* **89**, 022317 (2014).

[44] Y. Li and J. D. Thompson, High-Rate and High-Fidelity Modular Interconnects between Neutral Atom Quantum Processors, *PRX Quantum* **5**, 020363 (2024).

[45] S. Sunami, S. Tamiya, R. Inoue, H. Yamasaki, and A. Goban, Scalable Networking of Neutral-Atom Qubits: Nanofiber-Based Approach for Multiprocessor Fault-Tolerant Quantum Computers, *PRX Quantum* **6**, 010101 (2025).

[46] T. Đorđević, P. Samutpraphoot, P. L. Ocola, H. Bernien, B. Grinkemeyer, I. Dimitrova, V. Vuletić, and M. D. Lukin, Entanglement transport and a nanophotonic interface for atoms in optical tweezers, *Science* **373**, 1511 (2021).

[47] S. G. Menon, N. Glachman, M. Pompili, A. Dibos, and H. Bernien, An integrated atom array-nanophotonic chip platform with background-free imaging, *Nature Communications* **15**, 6156 (2024).

[48] P. L. Ocola, I. Dimitrova, B. Grinkemeyer, E. Guardado-Sánchez, T. Đorđević, P. Samutpraphoot, V. Vuletić, and M. D. Lukin, Control and Entanglement of Individual Rydberg Atoms near a Nanoscale Device, *Physical Review Letters* **132**, 113601 (2024).

[49] D. Hunger, T. Steinmetz, Y. Colombe, C. Deutsch, T. W. Hänsch, and J. Reichel, A fiber Fabry–Perot cavity with high finesse, *New Journal of Physics* **12**, 065038 (2010).

[50] J. Ningyuan, A. Georgakopoulos, A. Ryou, N. Schine, A. Sommer, and J. Simon, Observation and characterization of cavity Rydberg polaritons, *Physical Review A* **93**, 041802 (2016).

[51] T. Stoltz, H. Hegels, M. Winter, B. Röhr, Y.-F. Hsiao, L. Husel, G. Rempe, and S. Dürr, Quantum-Logic Gate between Two Optical Photons with an Average Efficiency above 40%, *Physical Review X* **12**, 021035 (2022).

[52] J. Vaneeckloo, S. Garcia, and A. Ourjoumtsev, Intracavity Rydberg Superatom for Optical Quantum Engineering: Coherent Control, Single-Shot Detection, and Optical π Phase Shift, *Physical Review X* **12**, 021034 (2022).

[53] Y. O. Dudin, L. Li, F. Bariani, and A. Kuzmich, Observation of coherent many-body Rabi oscillations, *Nature Physics* **8**, 790 (2012).

[54] J. Zeiher, P. Schauß, S. Hild, T. Macrì, I. Bloch, and C. Gross, Microscopic Characterization of Scalable Coherent Rydberg Superatoms, *Physical Review X* **5**, 031015 (2015).

[55] F. Nogrette, H. Labuhn, S. Ravets, D. Barredo, L. Béguin, A. Vernier, T. Lahaye, and A. Browaeys, Single-atom trapping in holographic 2d arrays of microtraps with arbitrary geometries, *Phys. Rev. X* **4**, 021034 (2014).

[56] H. Tanji-Suzuki, I. D. Leroux, M. H. Schleier-Smith, M. Cetina, A. T. Grier, J. Simon, and V. Vuletić, Chapter 4 - interaction between atomic ensembles and optical resonators: Classical description, in *Advances in Atomic, Molecular, and Optical Physics*, Vol. 60 (Academic Press, 2011) pp. 201–237.

[57] A. Periwal, E. S. Cooper, P. Kunkel, J. F. Wienand, E. J. Davis, and M. Schleier-Smith, Programmable interactions and emergent geometry in an array of atom clouds, *Nature* **600**, 630 (2021).

[58] H. Levine, D. Bluvstein, A. Keesling, T. T. Wang, S. Ebadi, G. Semeghini, A. Omran, M. Greiner, V. Vuletić, and M. D. Lukin, Dispersive optical systems for scalable raman driving of hyperfine qubits, *Physical Review A* **105**, 032618 (2022).

[59] M. P. van Exter, M. Wubs, E. Hissink, and C. Koks, Fine structure in Fabry-Perot microcavity spectra, *Physical Review A* **106**, 013501 (2022).

[60] J. Post, C. He, C. Koks, R. van Velzen, A. Corazza, Y. L. Fontana, M. Erbe, R. J. Warburton, and M. P. van Exter, Optical microcavity characterization via resonance spectra and modes, *Physical Review A* **112**, 033537 (2025).

[61] Z. Yan, J. Ho, Y.-H. Lu, S. J. Masson, A. Asenjo-Garcia, and D. M. Stamper-Kurn, Superradiant and subradiant cavity scattering by atom arrays, *Phys. Rev. Lett.* **131**, 253603 (2023).

[62] A. Osterwalder and F. Merkt, Using high rydberg states as electric field sensors, *Phys. Rev. Lett.* **82**, 1831 (1999).

[63] J. A. Sedlacek, A. Schwettmann, H. Kübler, R. Löw, T. Pfau, and J. P. Shaffer, Microwave electrometry with rydberg atoms in a vapour cell using bright atomic resonances, *Nature Physics* **8**, 819 (2012).

[64] S. de Léséleuc, D. Barredo, V. Lienhard, A. Browaeys, and T. Lahaye, Analysis of imperfections in the coherent optical excitation of single atoms to Rydberg states, *Physical Review A* **97**, 053803 (2018).

[65] X. Jiang, J. Scott, M. Friesen, and M. Saffman, Sensitivity of quantum gate fidelity to laser phase and intensity noise, *Physical Review A* **107**, 042611 (2023).

[66] T. Denecker, Y. T. Chew, O. Guillemant, G. Watanabe, T. Tomita, K. Ohmori, and S. de Léséleuc, Measurement and feedforward correction of the fast phase noise of lasers, *Physical Review A* **111**, 042614 (2025).

[67] R. Raussendorf and H. J. Briegel, A One-Way Quantum Computer, *Physical Review Letters* **86**, 5188 (2001).

[68] J. Borregaard, P. Kómár, E. M. Kessler, A. S. Sørensen, and M. D. Lukin, Heralded Quantum Gates with Integrated Error Detection in Optical Cavities, *Physical Review Letters* **114**, 110502 (2015).

[69] W. Chen, J. Hu, Y. Duan, B. Braverman, H. Zhang, and V. Vuletić, Carving Complex Many-Atom Entangled States by Single-Photon Detection, *Physical Review Letters* **115**, 250502 (2015).

[70] J. Ramette, J. Sinclair, Z. Vendeiro, A. Rudelis, M. Cetina, and V. Vuletić, Any-To-Any Connected Cavity-Mediated Architecture for Quantum Computing with Trapped Ions or Rydberg Arrays, *PRX Quantum* **3**, 010344 (2022).

[71] J. Ramette, J. Sinclair, Z. Li, and V. Vuletić, Carving entangled multiparticle states with exponentially improved fidelity, *Physical Review A* **111**, 052426 (2025).

[72] S. E. Economou, N. Lindner, and T. Rudolph, Optically Generated 2-Dimensional Photonic Cluster State from Coupled Quantum Dots, *Physical Review Letters* **105**, 093601 (2010).

[73] O. Rubies-Bigorda, S. J. Masson, S. F. Yelin, and A. Asenjo-Garcia, Deterministic Generation of Photonic Entangled States Using Decoherence-Free Subspaces, *Physical Review Letters* **134**, 213603 (2025).

[74] J. Gelhausen, M. Buchhold, A. Rosch, and P. Strack, Quantum-optical magnets with competing short- and long-range interactions: Rydberg-dressed spin lattice in an optical cavity, *SciPost Physics* **1**, 004 (2016).

- [75] J. Rohn, M. Hörmann, C. Genes, and K. P. Schmidt, Ising model in a light-induced quantized transverse field, *Physical Review Research* **2**, 023131 (2020).
- [76] X.-F. Zhang, Q. Sun, Y.-C. Wen, W.-M. Liu, S. Eggert, and A.-C. Ji, Rydberg Polaritons in a Cavity: A Superradiant Solid, *Physical Review Letters* **110**, 090402 (2013).
- [77] H. Hosseiniabadi, R. J. Valencia-Tortora, A. N. Mikheev, D. E. Chang, J. Zeiher, R. Moessner, and J. Marino, The $(PXP)^2$ model: Long-range quantum scars in optical cavities, arXiv:2510.02246 (2025).
- [78] C.-R. Mann, M. A. Oehlgrien, B. Jaworowski, G. Calajó, J. Marino, K. S. Choi, and D. E. Chang, Squeezing Classical Antiferromagnets into Quantum Spin Liquids via Global Cavity Fluctuations, arXiv:2512.05630 (2025).